RSC Advances

PAPER

View Article Online
View Journal | View Issue

Cite this: *RSC Adv.*, 2022, **12**, 14321

Amino acids with fluorescent tetrazine ethers as bioorthogonal handles for peptide modification†

Enric Ros,[a] Marina Bellido,[a] Joan A. Matarin,[ab] Albert Gallen,[c] Manuel Martínez,[cd] Laura Rodríguez,[cd] Xavier Verdaguer,[ae] Lluís Ribas de Pouplana[af] and Antoni Riera *[ae]

A set of 3-bromo-1,2,4,5-tetrazines with three distinct substitutions have been used as reagents for late-stage functionalization of small molecules through nucleophilic aromatic substitution. Spectroscopic studies of the products obtained proved that tetrazine ethers are intrinsically fluorescent. This fluorescence is lost upon inverse Electron-Demand Diels–Alder (iEDDA) cycloaddition with strained alkenes. Tetrazine-phenol ethers are rather interesting because they can undergo rapid iEDDA reactions with a second order rate constant (k_2) compatible with bioorthogonal ligations. As a showcase, L-tyrosine was derivatized with 3-bromo-6-methyl-1,2,4,5-tetrazine and coupled to the peptide drug octreotide. This peptide was detected in cellular flow cytometry, and its fluorescence turned off through a bioorthogonal iEDDA cycloaddition with a strained alkene, showing for the first time the detection and reactivity of intrinsically fluorescent tetrazines in a biologically relevant context. The synthesis and characterization of fluorescent tetrazine ethers with bioorthogonal applicability pave the way for the generation of useful compounds for both detection and bioconjugation *in vivo*.

Received 20th April 2022
Accepted 5th May 2022

DOI: 10.1039/d2ra02531k

rsc.li/rsc-advances

Introduction

Since the advent of "click chemistry"[1] at the beginning of the century, bioconjugation has experienced exponential growth. Click reactions fulfill the criteria of being simple and non-sensitive to oxygen and/or water and they yield clean final products. They can be used in biological contexts if other requirements are met, namely they must be unreactive towards the functional groups found in nature, display fast kinetics and not require catalysis or generate toxic entities. These click reactions are known as bioorthogonal.[2] In recent years, bioorthogonal reactions have found increasing applications in research and biomedical settings because they offer unique control over the reactivity of small molecules when applied in biological contexts.

Of the handful of bioorthogonal reactions reported to date, the most widely used is probably the tetrazine ligation with strained alkenes or alkynes through an inverse Electron-Demand Diels–Alder (iEDDA) cycloaddition.[3,4] These reactions have been used for drug delivery strategies,[5,6] *in vivo* prodrug activation,[7] novel drug discovery techniques[8] and pre-targeted PET imaging,[9] amongst many others.

In particular, one application that has attracted a huge interest is the development of fluorescent probes.[10] Indeed, over recent years, several tetrazine-conjugates with a range of fluorophores such as BODIPY,[11,12] coumarin,[13] xanthene,[14] phenoxazine,[15] siliconrhodamine,[16,17] naphthalene[18] or cyanine[19] derivatives have been developed. The fluorogenic character of these compounds after iEDDA reaction of the tetrazine core makes them advantageous for *in vivo* imaging experiments as they do not require washing steps, thus resulting in a "turn-on" fluorescent system.[20,21]

In contrast, although intrinsically fluorescent tetrazines are among the smallest organic fluorophores,[22] their use is far less common. To date, fluorescent tetrazines, initially reported in the 1960's,[23] are prepared mostly by nucleophilic aromatic substitution (S_NAr) on 3,6-dichlorotetrazine.[24] In this regard, both symmetrical and unsymmetrical ether-bridged tetrazines have been reported as well as their fluorescent and

[a]*Institute for Research in Biomedicine (IRB Barcelona), Barcelona Institute of Science and Technology, Baldiri Reixac 10, 08028 Barcelona, Spain. E-mail: antoni.riera@irbbarcelona.org*

[b]*BCN Peptides S.A., Pol. Ind. Els Vinyets-Els Fogars, Sector II, Ctra. Comarcal 244, Km. 22, 08777 Sant Quintí de Mediona, Barcelona, Spain*

[c]*Departament de Química Inorgànica i Orgànica, Secció Química Inorgànica. Universitat de Barcelona, Martí i Franquès 1, 08028 Barcelona, Spain*

[d]*Institut de Nanociència i Nanotecnologia (IN2UB), Universitat de Barcelona, 08028. Barcelona, Spain*

[e]*Departament de Química Inorgànica i Orgànica, Secció Química Orgànica. Universitat de Barcelona, Martí i Franquès 1, 08028 Barcelona, Spain*

[f]*Institució Catalana de Recerca i Estudis Avançats (ICREA), Passeig Lluís Companys 23, 08010 Barcelona, Spain*

† Electronic supplementary information (ESI) available: Characterization of new compounds and details of kinetic measurement. See https://doi.org/10.1039/d2ra02531k

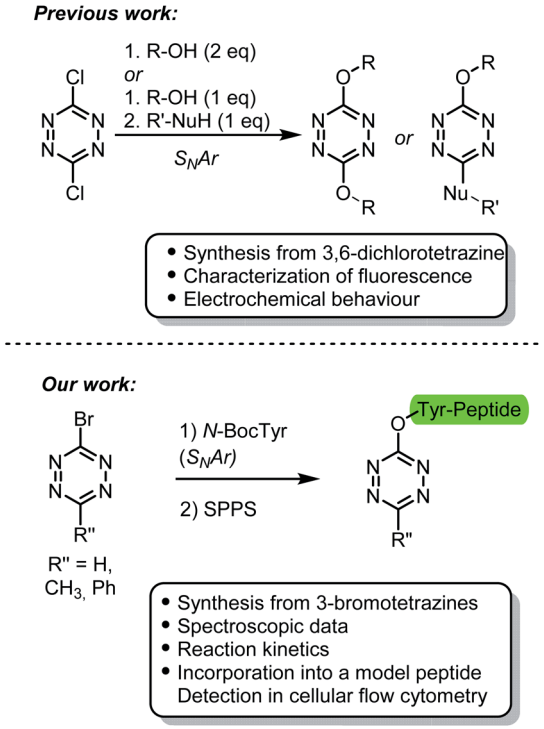

Fig. 1 Comparison between the characterization and application of tetrazine ethers previously reported and those presented herein.

electrochemical behaviour (Fig. 1, top).[25–27] However, there are no precedents in the exploitation of the emissive behavior and bioorthogonal reactivity of fluorescent tetrazines *in vivo.* This may be due to the slow reaction kinetics shown by the bis-substituted products.

When considering the reaction kinetics in iEDDA-type cycloadditions, the predominant factor is the energy gap between the HOMO (highest occupied molecular orbital) of the dienophile and LUMO (lowest unoccupied molecular orbital) of the diene.[28,29] Consequently, the presence of electron-donating groups (EDGs) in the tetrazine ring, which acts as the diene, decreases their reactivity by increasing the energy of the LUMO.[29] For S_NAr products of 3,6-dichlorotetrazine, the presence of two EDGs on the tetrazine probably leads to sluggish kinetics in the iEDDA cycloaddition, thus limiting their applicability in bioorthogonal reactions.

We and others, have previously reported the synthesis and use of 3-bromotetrazines as excellent electrophiles for S_NAr reactions.[30–32] We envisaged that we could exploit the reactivity of these compounds under mild conditions to easily generate asymmetrically substituted fluorescent tetrazine ethers. We anticipated that the reaction products would display faster kinetics in the iEDDA cycloaddition compared with those synthesized using 3,6-dichlorotetrazine as precursor. To this end, here we describe the synthesis of tyrosine derivatives bearing a tetrazine ether moiety. One of these amino acids was introduced into a model peptide, thereby showcasing its potential use as fluorescent probe capable to undergo bioorthogonal reactions *in vivo* (Fig. 1, bottom).

Results and discussion

Recent years have witnessed increasing interest in the use of different bromotetrazines for late-stage functionalization of small molecules or macromolecules, either through S_NAr reactions[30,31] or *via* Pd-catalyzed cross-coupling reactions (such as Stille[21] or Sonogashira[33]). Here we prepared the mono-substituted 3-bromo-1,2,4,5-tetrazine (**1a**), and the asymmetrically substituted 3-bromo-6-methyl-1,2,4,5-tetrazine (**1b**) and 3-bromo-6-phenyl-1,2,4,5-tetrazine (**1c**). We used a recently described and convenient synthetic route, that gave the highest overall yields (12–15%) reported to date.[31,33] We selected **1b** for the first screening of nucleophiles. As expected, tetrazine **1b** reacted rapidly and in quantitative yields with aliphatic and aromatic amines to give the secondary amines **2a** and **2b**; with alcohols to give the ethers **2c** and **2d**; and with thiols to give the sulfides **2e** and **2f** (Table 1).

To determine the emission behaviour of the heteroatom-substituted tetrazines resulting from these reactions, we registered the UV-Vis spectra of compounds **2a–f**. They all showed an absorption band (λ_{Abs}) in the 530–540 nm region, which is characteristic of tetrazines (Table 2; Fig. 2). Interestingly, only the tetrazine ethers prepared from alcohols or phenols (**2c** and **2d**) were found moderately emissive with quantum yields over 12% (Table 2) and emission band at 580–590 nm (Fig. 2). On the contrary, the substituted amines **2a–b** and sulfides **2e–f** were virtually non-emissive. As expected, the emission signals of **2c** and **2d** were lost when they were reacted with a strained dienophile, resulting in a fluorescence "turn-off" effect upon iEDDA reaction.

Although some intrinsically fluorescent tetrazines have been reported,[25–27] they have never been used as bioorthogonal probes *in vivo*. We envisaged that tetrazines similar to products **2c–d** could fulfill the criteria of fluorescence intensity, reactivity in the iEDDA cycloaddition, and stability in biological media, to be used under biocompatible conditions. To study these

Table 1 S_NAr reactions of 3-bromotetrazine **1b** with a set of aromatic and aliphatic amines, alcohols and thiols

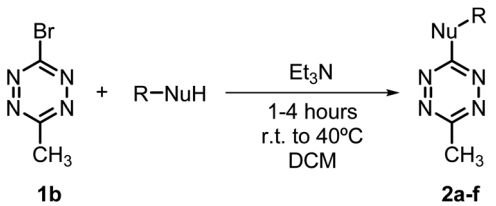

R-NuH		Yield
N-BocNH-$(CH_2)_3$-NH_2	**2a**	76%
p-MeO-C_6H_4-NH_2	**2b**	70%
N-BocNH-$(CH_2)_3$-OH	**2c**	79%
p-Cl-C_6H_4-OH	**2d**	92%
CH_3-$(CH_2)_{11}$-SH	**2e**	89%
p-F-C_6H_4-SH	**2f**	88%

Table 2 Spectroscopic data of heteroatom-substituted tetrazines in DCM (1 mM)

	λ_{max} (nm)	ε_{max} (M^{-1} cm^{-1})	λ_{em} (nm)	Φ_F (%)
2a	531	416	587	0.3
2b	533	303	572	0.6
2c	536	696	581	12.2
2d	539	688	588	12.4
2e	537	550	586	1.6
2f	537	554	593	1.0

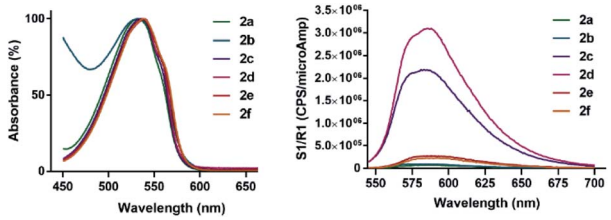

Fig. 2 Normalized absorption and emission spectra of compounds 2a–f.

parameters, we synthesized a set of unnatural amino acids containing the tetrazine ether functionality. These compounds were easily prepared by S_NAr reaction of **1a–c** with *N*-Boc-tyrosine, followed by Boc-deprotection with HCl 4 M to obtain amino acids **4a–c** as hydrochloride salts (Scheme 1). With the available tyrosine analogues, we characterized the emission intensity of compounds **4a–c** (Table 3). Somewhat surprisingly, compound **4b**, bearing a 4-methyltetrazinyl substituent, showed higher fluorescence than analogues **4a** and **4c.** We speculate that this difference may be due to the geometries of the products and the donor/acceptor properties of the different substituents in the tetrazine ether ring.

We then studied the reaction kinetics of amino acids **4a–c** in the iEDDA cycloaddition with the strained dienophile (*E*)-cyclooct-4-enol (**TCO-OH**) under pseudo first-order conditions in water : DMSO (4 : 1) at 37 °C (Scheme 5). The second-order

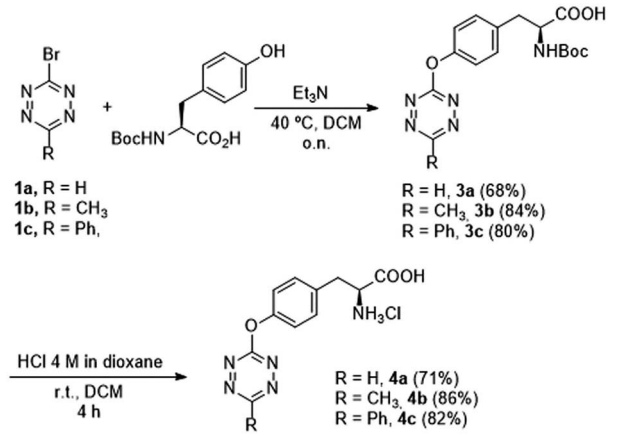

Scheme 1 Synthesis of L-tyrosine derivatives bearing fluorescent tetrazine ethers.

Table 3 Luminescence data of tyrosine derivatives 4a–c

	λ_{exc} (nm)	λ_{em} (nm)	Φ_F (%)
4a	520	572	7.58 ± 0.02
4b	531	587	11.9 ± 0.3
4c	532	581	7.08 ± 0.01

rate constants (k_2) are shown in Fig. 3. As expected, the mono-substituted tetrazine **4a** undergoes cycloaddition 14 times faster than the methyl analogue **4b**, whereas the phenyl substituted tetrazine **4c** was three times faster than **4b**. The rate enhancements are clearly attributed to a combination of electronic and steric effects[34,35] and confirms the high reactivity of mono-substituted tetrazines. Despite the moderate values obtained, when compared with certain tetrazines substituted with electron-withdrawing groups (EWGs), the second-order rate constants are in the range of some of the most commonly used bioorthogonal reactions.

Given the moderate but significant fluorescence quantum yield (11.89 ± 0.25) for **4b**, we decided to proceed our studies with this compound, despite showing the slowest k_2 of all three compounds (29.6 M^{-1} s^{-1}). Consequently, we determined the stability of **4b** in fetal bovine serum (FBS) at 37 °C, thus mimicking physiological conditions. By monitoring the absorbance decay at the specific wavelength of the tetrazine ring over time, we found that more than 50% of tetrazine **4b** remained intact after 48 h of incubation (see ESI†). The excitation wavelength of **4b** (λ_{Exc} = 531 nm) ensured minimal absorption overlap with endogenous chromophores and the absence of major scattering effects, both events known to interfere with fluorophores excited at shorter wavelengths (<500 nm) when used in a biological context.[36,37] We hypothesized that this advantage could counterbalance the moderate fluorescence quantum yield displayed by **4b**. We concluded that **4b** presents the necessary trade-off between stability and reactivity to be used *in vivo*.[38]

Octreotide is a marketed drug with high affinity for Somatostatin receptor type 2 (SSTR2) that is used to treat several endocrine disorders.[39] To showcase the potential of **4b** in

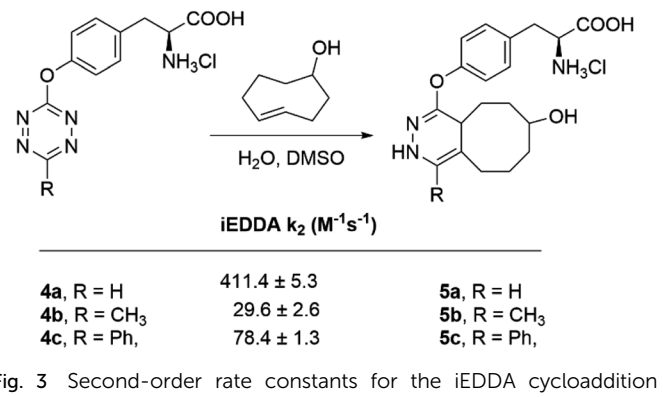

Fig. 3 Second-order rate constants for the iEDDA cycloaddition between L-tyrosine derivatives (**4a–c**) and **TCO-OH** in water : DMSO (4 : 1) at 37 °C.

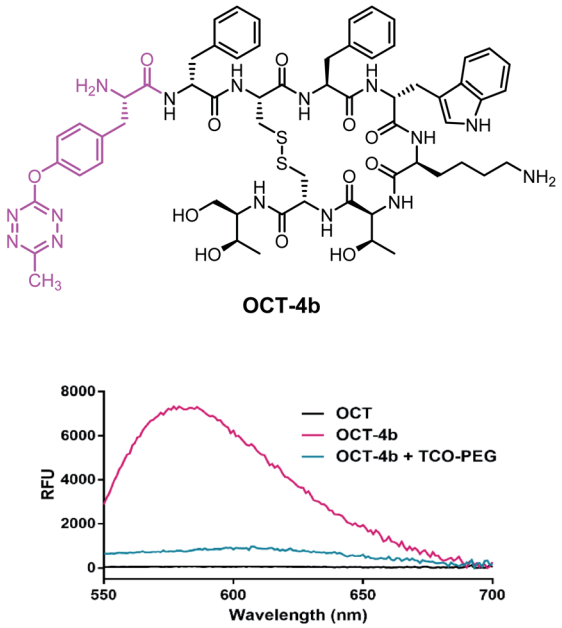

Fig. 4 (a) Structure of OCT-4b; (b) emission spectra of OCT, OCT-4b and the iEDDA cycloaddition product of OCT-4b with TCO-PEG.

a biologically relevant setting, we synthesized an octreotide (OCT)[40] derivative by coupling the *N*-Boc protected intermediate **3b** to its N-terminal residue by solid-phase peptide synthesis (SPPS). After cleavage of the corresponding resin and removal of the protecting groups, **OCT-4b** (Fig. 4a) was obtained and purified by preparative HPLC. As expected, the spectroscopic characteristics of **OCT-4b** (λ_{Abs} = 513 nm and λ_{Em} = 579 nm) matched those observed for **4b** alone, and the fluorescence was equally lost after iEDDA reaction with **TCO-PEG**, a water soluble version of **TCO-OH** (Fig. 4b).

To study whether the intrinsic tetrazine fluorescence can be detected in a biologically relevant context, **OCT-4b** was then incubated with CHO–K1 cells overexpressing SSTR2. After the necessary time for internalization, the excess culture medium was removed and cells were monitored by flow cytometry (Fig. 5a). The density plots obtained showed a clear increase in the total relative fluorescence of the samples treated with **OCT-4b** compared to the control cells treated with **OCT** alone. Moreover, no differences were observed between the side scatter *vs.* forward scatter plots in both conditions, therby indicating that there was no toxicity related to the use of **4b**.

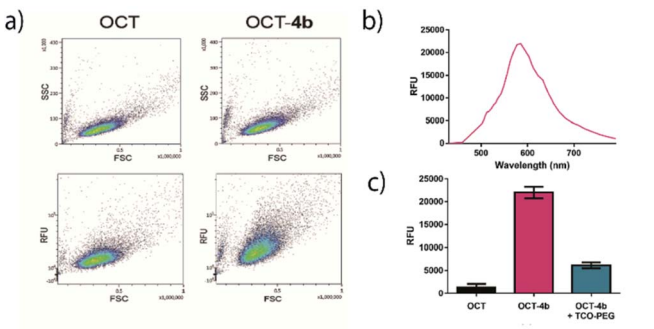

Fig. 5 (a) Flow cytometry plots of CHO–K1 cells treated with OCT and OCT-4b. (b) Mean emission spectrum of cells treated with OCT-4b; (c) quantification of the emission signal of cells treated with OCT, OCT-4b and OCT-4b + TCO-PEG at the maximum emission wavelength (585.3 nm). (SSC = Side Scatter; FSC = Forward Scatter; RFU = Relative Fluorescence Units).

To demonstrate that the increased fluorescence was caused by the tetrazine ether in **4b**, the averaged emission spectra of cells were calculated and plotted (Fig. 5b). Indeed, the emission maximum of **OCT-4b** treated cells (λ_{em} = 585 nm) were consistent with the emission of tetrazine ethers. Finally, to validate that the reaction kinetics of **4b** are suitable to undergo *in vivo* iEDDA cycloadditions, we incubated **OCT-4b** treated cells with **TCO-PEG** for 30 min. Gratifyingly, we observed that the fluorescence at the maximum emission wavelength returned to near-basal levels, thereby indicating that the reaction was taking place, and fluorescence was subsequently lost after iEDDA cycloaddition *in vivo* (Fig. 5c).

Experimental

1. Synthesis of 3-bromotetrazines

3-Bromotetrazines **1a–c** were prepared following the described procedures.[31,33]

2. General procedure for the S_NAr reaction with aliphatic and aromatic nucleophiles

Bromo tetrazine **1a** (30 mg, 0.171 mmol, 1.0 eq.) and the corresponding **R-NuH** (0.206 mmol, 1.2 eq.) were placed in a sealed vial, which was degassed and placed under N_2 atmosphere. Anhydrous DCM (1 mL, 0.17 M) was then added, followed by Et_3N (24 μL, 0.17 mmol, 1.0 eq.). The mixture was stirred for 1–4 h until completion of the reaction was confirmed by TLC. For alcohol substitutions, the reaction mixture was heated at 40 °C to reach completion.

The reaction mixtures were then concentrated under reduced pressure, diluted in water and extracted with DCM three times. The combined organic layers were dried over $MgSO_4$ and evaporated under vacuum. Purification by flash column chromatography was performed using hexanes with increasing ethyl acetate (EtOAc) concentrations to afford **2a–f**.

2.1 *N*-Boc-*O*-(6-methyl-1,2,4,5-tetrazin-3-yl)-3-amino-propanol (2c). Pink oil (36.5 mg, 79%). ^{1}H NMR (400 MHz, $CDCl_3$; TMS) δ 4.68 (2H, t, J = 6.2 Hz, –CH_2O–), 3.37 (2H q, J = 6.4 Hz, –CH_2N–), 2.99 (3H, s, CH_3), 2.12 (2H, p, J = 6.4 Hz, –CH_2–), 1.43 (9H, d, J = 4.9 Hz, *t*-Bu) ppm. ^{13}C NMR (101 MHz, $CDCl_3$) δ 166.8, 165.5, 156.1, 67.4, 37.5, 32.0, 29.4, 28.5, 20.3 ppm. HRMS (ESI$^+$) calculated for $C_{11}H_{20}O_3N_5$ [M + H]$^+$: 270.15607/ found 270.15602. IR (KBr) υ_{max}: 3360 (NH), 2960 (CH), 2920 (CH) cm^{-1}. λ_{Abs} = 536 nm, ε = 696 M^{-1} cm^{-1}, λ_{Em} = 581 nm, Φ_F = 12%.

2.2 3-(4-Chlorophenoxy)-6-methyl-1,2,4,5-tetrazine (2d). Pink solid (34.4 mg, 92%). M_p (hexane, EtOAc) = 90.2 °C. ^{1}H NMR (400 MHz, $CDCl_3$) δ 7.47–7.41 (2H, m, Ar), 7.25–7.19 (2H, m, Ar), 3.04 (3H, s, CH_3) ppm. ^{13}C NMR (101 MHz, $CDCl_3$; TMS) δ 167.6, 166.6, 150.4, 132.0, 130.2, 122.4, 20.3 ppm. HRMS (ESI$^+$)

calculated for $C_9H_8ClN_4O$ $[M+H]^+$: 223.0381/found 223.0383. IR (KBr) υ_{max}: 3095 (CH), 2918 (CH) cm^{-1}. $\lambda_{Abs} = 538$ nm, $\varepsilon = 688$ $M^{-1}cm^{-1}$, $\lambda_{Em} = 588$ nm, $\Phi_F = 12\%$.

3. Synthesis of tetrazine-containing tyrosine derivatives

3.1 General procedure of the S_NAr reaction between 1a–c and N^{α}-Boc-L-tyrosine. N^{α}-Boc-L-tyrosine (77.0 mg, 0.274 mmol, 1.2 eq.) and the corresponding bromo tetrazine (**1a**, **1b** or **1c**, 0.228 mmol, 1 eq.) were dissolved in 2.0 mL DCM, and Et_3N (32 μL, 0.228 mmol, 1 eq.) was added. The mixture was stirred overnight at 40 °C, at which point TLC showed completion of the reaction.

The reaction mixtures were concentrated under reduced pressure, diluted in HCl 0.1 M aqueous solution and extracted with DCM three times. The combined organic layers were dried over $MgSO_4$ and evaporated under vacuum. Purification by flash column chromatography was performed in DCM with 1% acetic acid, with increasing concentrations of MeOH, to afford **3a–c**.

3.2 N^{α}-Boc-4-(6-methyl-1,2,4,5-tetrazin-3-yl)-L-tyrosine (3b). Pink gum (71.9 mg, 84%). ^{1}H NMR (400 MHz, $CDCl_3$; TMS) δ 7.30 (2H, d, $J = 8.5$ Hz, Ar), 7.23–7.19 (2H, d, Ar), 5.02 (1H, d, $J = 8.0$ Hz, NH), 4.64 (1H, m, CH), 3.29–3.05 (2H, m, CH_2), 3.03 (3H, s, CH_3), 1.43 (9H, s, *t*-Bu) ppm. ^{13}C NMR (101 MHz, $CDCl_3$) δ 175.6, 167.8, 166.4, 155.5, 151.2, 134.6, 131.2, 121.1, 80.6, 54.3, 37.4, 28.4, 20.4 pp. HRMS (ESI^+) calculated for $C_{17}H_{21}N_5O_5$ $[M+Na]^+$: 398.14349/found 398.14387.

3.3. N^{α}-Boc carbamate deprotection. General procedure. *N*-Boc amino acids **3a–c** were placed in a sealed vial, which was subsequently degassed. They were then placed under N_2 atmosphere, and dissolved in DCM at a final concentration of 0.2 M. HCl 4 M in dioxane (for a total of 2 eq. of HCl) was added. After stirring 4 hours at room temperature, the resulting solid was filtered over a glass filter crucible to obtain the desired products **4a–c**.

3.4 4-(6-Methyl-1,2,4,5-tetrazin-3-yl)-L-tyrosine hydrochloride (4b). Pink solid (28.6 mg, 86% starting from 40.0 mg of **3b**). ^{1}H NMR (400 MHz, CD_3OD; TMS) δ 7.48–7.43 (2H, d, Ar), 7.37–7.32 (2H, d, Ar), 4.31 (1H, dd, $J = 8.1$, 5.3 Hz, CH), 3.41 (1H, dd, $J = 14.5$, 5.3 Hz, CH), 3.21 (1H, dd, $J = 14.6$, 8.1 Hz, CH), 2.97 (3H, s, CH_3) ppm. ^{13}C NMR (101 MHz, CD_3OD) δ 171.1, 169.3, 167.7, 153.4, 134.1, 132.3, 122.9, 55.2, 36.7, 20.12 ppm. HRMS (ESI^+) calculated for $C_{12}H_{13}N_5O_3$ $[M+H]^+$: 276.1091/found 276.1091. IR υ_{max}: 3200 (OH and NH), 2912 (CH), 2863 (CH) cm^{-1}. λ_{Abs}: 531 nm.

4. Synthesis of OCT-4b by SPPS

OCT-resin was prepared by standard SPPS on a 2-chlorotrityl resin following the Fmoc/*t*Bu strategy.

Starting from 5.0 g of 2-Cl-Trt resin (1.60 mmol g^{-1}) and using Fmoc-L-threoninol (1 eq.) as the first amino acid. After Fmoc-removal of the last amino acid (Fmoc-D-Phe-OH) the resin was dried. Peptidyl resin (11.6 g, $f = 0.338$ mmol g^{-1}) was obtained and **OCT** was cleaved from the resin using a deprotection cocktail of TFA : dodecanethiol : thioanisole : triisopropylsilane : H_2O (85 : 6 : 3 : 3 : 3 v/v/v/v/v) for 2 h. The formation of the disulfide bridge was achieved by air oxidation dissolving the crude peptide in a mixture of H_2O : DMSO : AcOH (80 : 10 : 10 v/v/v) and stirring overnight. DMSO was removed through a polyaromatic adsorbent resin column chromatography.

OCT-4b was synthesized from peptidyl resin (**OCT**-resin) (1 eq., 0.14 mmol, 0.42 g) and **3b** (1.5 eq., 0.21 mmol, 0.08 g) using PyBOP/HOBt/DIEA (1.5eq./1.5eq./3eq.) as coupling reagents in DMF for 24 h. Reactivation with PyBOP/HOBt/DIEA was carried out for 20 h to achieve reaction completion. Peptidyl resin (**OCT-4b**-resin) (0.46 g) was obtained and subsequently cleaved and deprotected with TFA cocktail to obtain the reduced version of the peptide, which was air-oxidized in H_2O : DMSO : AcOH for 15 h. Then, DMSO was removed to finally obtain **OCT-4b**.

ESI-MS: calculated for $C_{49}H_{69}N_{10}O_{10}S_2$ $[M]^+$: 1021.3; found: 1021.3.

5. Absorbance spectra acquisition

Absorption spectra of compounds **2a–f** (in DCM) and **4a–c** (in methanol) at a final concentration of 1 mM were recorded on a Varian Cary 100 Bio UV spectrophotometer.

6. Fluorescence spectra acquisition

Fluorescence emission spectra of compounds **2a–f** (in DCM) and **4a–c** (in methanol) were recorded on a Horiba-Jobin-Ybon SPEX Nanolog spectrofluorimeter from dilute solutions with an absorbance value of 0.2 AU at the excitation wavelength (λ_{Ex}).

7. Quantum yield determination

Quantum yields of compounds **2a–f** (in DCM) and **4a–c** (in methanol) were acquired on a Quantaurus-QY Absolute PL spectrometer at the excitation wavelength (λ_{Ex}), using the specified solvent in each case as the reference solution.

8. Determination of iEDDA rate constants

The observed reaction rate constants were measured at 37 °C varying concentrations of **TCO-OH** under pseudo first-order conditions (**TCO-OH** being in a 10 to 50 fold excess). The kinetic full spectra profiles were monitored by time-resolved UV-Vis spectroscopy in the 700–200 nm range. The time-resolved spectral changes have been quantified using ReactLab or Specfit software as a single step kinetics.[41,42] Second-order rate constants were standardly derived[43] from the slopes of the k_{obs} *vs.* [TCO-OH] plots (see ESI†).

9. Stability of 4b in FBS *via* UV-Vis spectroscopy

4b was dissolved in FBS (Merck) at a final concentration of 1 mM, and incubated at 37 °C for a total of 48 h in a flat-bottomed 96-well plate. Absorbance measurements were taken at $\lambda = 510$ nm at different time points ($t = 0.5$ h, 1 h, 2 h, 4 h, 6 h, 8 h, 24 h and 48 h).

10. Cellular flow cytometry

Chinese Hamster Ovary K1 (CHO-K1) cells overexpressing SSTR2 cells were grown in Kaighn's modification of Ham's F-12K medium (F-12K, ThermoFisher Scientific) supplemented

with 10% FBS, 25 mM HEPES, 100 U mL^{-1} penicillin, 100 μg mL^{-1} streptomycin and 200 μg mL^{-1} geneticin at 37 °C and 5% CO_2.

For flow cytometry studies, cells at 70–80% confluence were incubated with a solution of **OCT**, **OCT-4b** or **OCT-4b-TCO-PEG** in water at a final concentration of 250 μM for 14 h in flat-bottomed 24-well plates with 500 μL of culture medium. The medium was then removed and cells were washed with PBS once and fresh medium was added. In the cases were **TCO-PEG** was added (**OCT-4b** + **TCO-PEG**), 10 μL from a 50 mM solution in water was added (final concentration of 1 mM) for 30 minutes.

Cells were then trypsinized, quantified (1.1×10^6 total cells), washed with PBS once and resuspended in PBS at a final concentration of 1.5×10^6 cells per mL. They were then processed in a SA3800 Spectral Cell Analyzer (Sony Biotechnology) with excitation at 488 nm (Window Extension Normal, threshold CH=FSC, threshold value 16.7%, FSC gain = 10, SSC voltage 27%, fluorescence PMT voltage 85%).

Conclusions

We have reported that 3-bromotetrazines are excellent electrophilic reagents to undergo S_NAr reactions with heteroatoms acting as nucleophiles. The previously reported improved syntheses of **1a–c** provides a facile and efficient method for late-stage tetrazine functionalization of small molecules.

The corresponding oxygen-substituted tetrazines derived from alcohols or phenols showed a remarkable fluorescent behavior that is not present in the nitrogen or sulphur analogues. Such fluorescence is lost after the corresponding iEDDA reaction.

To showcase the applicability of tetrazine ethers in biologically relevant settings, we have functionalized the phenol contained in L-Tyrosine with **1a–c**. Quantum yield determination of the obtained products revealed that the 6-methyltetrazin-3-yl analog **4b** showed the strongest emissive properties, with an excitation wavelength that ensured minimal interference with endogenous chromophores. In addition, its second order rate constant for the subsequent iEDDA cycloaddition with a strained alkene was in line with some of the commonly used bioorthogonal ligations. Moreover, we demonstrated that **4b** is also stable under physiological conditions for several days.

Consequently, we used the 6-methyltetrazin-3-yl tyrosine ether to modify a therapeutically relevant peptide (**OCT-4b**) and used it in cell flow cytometry, where we could "turn-off" its fluorescence upon reaction with a strained dienophile. Thus, we demonstrate for the first time that the intrinsic fluorescence of tetrazine ethers can be detected in a biological relevant context, and that the reaction kinetics of such compounds is suitable to undergo bioorthogonal iEDDA cycloadditions *in vivo*.

In summary, herein we report a strategy to achieve fluorescent tetrazine ethers that can be used as bioconjugation handles *in vivo.* The straightforward synthesis of tetrazine ethers from the reaction of **1a–c** with alcohols or phenols, together with their fluorescent behaviour, bioorthogonal reactivity, stability in physiological conditions and small size are clear advantages for the generation of useful chemical biology tools with multiple applications.

Our future efforts will focus on incorporating the reported tetrazine ethers into other biologically relevant molecules, such as proteins through genetic code expansion methodologies. Alternatively, we anticipate that these compounds could serve to generate quantifiable fluorescent probes able to switch off their emissive properties upon iEDDA cycloaddition *in vivo*.

Author contributions

Conceptualization and writing: E. R. and A. R. Supervision and funding acquisition: A. R., L. RdP., X. V.; experimental: E. R., M. B., J. A. M. and A. G. Reaction kinetics: A. G., M. M.; optical measurements: E. R., L. R. All authors have read and agreed to the published version of the manuscript.

Conflicts of interest

There are no conflicts to declare.

Acknowledgements

This research was funded by the Spanish Ministerio de Ciencia e Innovación (MCINN), grant numbers PID2020-115074GB-I00 to A. R. and X. V., PID2019-104121GB-I00 to L. R. and PID2019-108037RB-100 to L. R.dP. We also acknowledge institutional funding from MINECO through the Centers of Excellence Severo Ochoa Award given to IRB Barcelona, as well as from the CERCA Program of the Generalitat de Catalunya. L.R.dP is an ICREA Programme Investigator.

Notes and references

1 H. C. Kolb, M. G. Finn and K. B. Sharpless, *Angew. Chem., Int. Ed.*, 2001, **40**, 2004–2021.
2 E. M. Sletten and C. R. Bertozzi, *Angew. Chem., Int. Ed.*, 2009, **48**, 6974–6998.
3 B. L. Oliveira, Z. Guo and G. J. L. Bernardes, *Chem. Soc. Rev.*, 2017, **46**, 4895–4950.
4 H. Wu and N. K. Devaraj, *Acc. Chem. Res.*, 2018, **51**, 1249–1259.
5 R. M. Versteegen, R. Rossin, W. Ten Hoeve, H. M. Janssen and M. S. Robillard, *Angew. Chem., Int. Ed.*, 2013, **52**, 14112–14116.
6 R. Rossin, S. M. J. Van Duijnhoven, W. Ten Hoeve, H. M. Janssen, L. H. J. Kleijn, F. J. M. Hoeben, R. M. Versteegen and M. S. Robillard, *Bioconjugate Chem.*, 2016, **27**, 1697–1706.
7 H. Lebraud, D. J. Wright, C. N. Johnson and T. D. Heightman, *ACS Cent. Sci.*, 2016, **2**, 927–934.
8 A. Rutkowska, D. W. Thomson, J. Vappiani, T. Werner, K. M. Mueller, L. Dittus, J. Krause, M. Muelbaier, G. Bergamini and M. Bantscheff, *ACS Chem. Biol.*, 2016, **11**, 2541–2550.

9 C. Denk, D. Svatunek, T. Filip, T. Wanek, D. Lumpi, J. Fröhlich, C. Kuntner and H. Mikula, *Angew. Chem., Int. Ed.*, 2014, **53**, 9655–9659.
10 G. B. Cserép, A. Herner and P. Kele, *Methods Appl. Fluoresc.*, 2015, **3**, 042001.
11 N. K. Devaraj, S. Hilderbrand, R. Upadhyay, R. Mazitschek and R. Weissleder, *Angew. Chem., Int. Ed.*, 2010, **49**, 2869–2872.
12 A. Wieczorek, T. Buckup and R. Wombacher, *Org. Biomol. Chem.*, 2014, **12**, 4177–4185.
13 L. G. Meimetis, J. C. T. Carlson, R. J. Giedt, R. H. Kohler and R. Weissleder, *Angew. Chem., Int. Ed.*, 2014, **53**, 7531–7534.
14 H. Wu, J. Yang, J. Šečkute and N. K. Devaraj, *Angew. Chem., Int. Ed.*, 2014, **53**, 5805–5809.
15 G. Knorr, E. Kozma, A. Herner, E. A. Lemke and P. Kele, *Chem.–Eur. J.*, 2016, **22**, 8972–8979.
16 E. Kozma, G. Estrada Girona, G. Paci, E. A. Lemke and P. Kele, *Chem. Commun.*, 2017, **53**, 6696–6699.
17 P. Werther, K. Yserentant, F. Braun, N. Kaltwasser, C. Popp, M. Baalmann, D. P. Herten and R. Wombacher, *Angew. Chem., Int. Ed.*, 2020, **59**, 804–810.
18 D. Kim, J. H. Lee, J. Y. Koo, H. M. Kim and S. B. Park, *Bioconjugate Chem.*, 2020, **31**, 1545–1550.
19 G. Knorr, E. Kozma, J. M. Schaart, K. Németh, G. Török and P. Kele, *Bioconjugate Chem.*, 2018, **29**, 1312–1318.
20 A. Vázquez, R. Dzijak, M. Dračínský, R. Rampmaier, S. J. Siegl and M. Vrabel, *Angew. Chem., Int. Ed.*, 2017, **56**, 1334–1337.
21 A. Wieczorek, P. Werther, J. Euchner and R. Wombacher, *Chem. Sci.*, 2017, **8**, 1506–1510.
22 F. Miomandre and P. Audebert, *J. Photochem. Photobiol., C*, 2020, **44**, 100372.
23 M. A. El-Sayed, *J. Chem. Phys.*, 1963, **38**, 2834–2838.
24 P. Audebert, F. Miomandre, G. Clavier, M. C. Verniéres, S. Badré and R. Méallet-Renault, *Chem.–Eur. J.*, 2005, **11**, 5667–5673.
25 Q. Zhou, P. Audebert, G. Clavier, F. Miomandre and J. Tang, *RSC Adv.*, 2014, **4**, 7193–7195.
26 Z. Qing, P. Audebert, G. Clavier, F. Miomandre, J. Tang, T. T. Vu and R. Méallet-Renault, *J. Electroanal. Chem.*, 2009, **632**, 39–44.
27 E. Jullien-Macchi, V. Alain-Rizzo, C. Allain, C. Dumas-Verdes and P. Audebert, *RSC Adv.*, 2014, **4**, 34127–34133.
28 J. M. J. M. Ravasco and J. A. S. Coelho, *J. Am. Chem. Soc.*, 2020, **142**, 4235–4241.
29 R. A. A. Foster and M. C. Willis, *Chem. Soc. Rev.*, 2013, **42**, 63–76.
30 S. D. Schnell, L. V. Hoff, A. Panchagnula, M. H. H. Wurzenberger, T. M. Klapötke, S. Sieber, A. Linden and K. Gademann, *Chem. Sci.*, 2020, **11**, 3042–3047.
31 E. Ros, M. Bellido, X. Verdaguer, L. Ribas de Pouplana and A. Riera, *Bioconjugate Chem.*, 2020, **31**, 933–938.
32 A. Counotte-Potman and H. C. Van Der Plas, *J. Heterocycl. Chem.*, 1981, **18**, 123–127.
33 E. Ros, A. Prades, D. Forson, J. Smyth, X. Verdaguer, L. R. de Pouplana and A. Riera, *Chem. Commun.*, 2020, **56**, 11086–11089.
34 J. Yang, Y. Liang, J. Šečkutė, K. N. Houk and N. K. Devaraj, *Chem.–Eur. J.*, 2014, **20**, 3365–3375.
35 J. A. Wagner, D. Mercadante, I. Nikić, E. A. Lemke and F. Gräter, *Chem.–Eur. J.*, 2015, **21**, 12431–12435.
36 B. F. Buksh, S. D. Knutson, J. V. Oakley, N. B. Bissonnette, D. G. Oblinsky, M. P. Schwoerer, C. P. Seath, J. B. Geri, F. P. Rodriguez-Rivera, D. L. Parker, G. D. Scholes, A. Ploss and D. W. C. MacMillan, *J. Am. Chem. Soc.*, 2022, **144**, 6154–6162.
37 C. Ash, M. Dubec, K. Donne and T. Bashford, *Lasers Med. Sci.*, 2017, **32**, 1909–1918.
38 A. C. Knall and C. Slugovc, *Chem. Soc. Rev.*, 2013, **42**, 5131–5142.
39 C. Bruns, F. Raulf, D. Hoyer, J. Schloos, H. Lübbert and G. Weckbecker, *Metabolism*, 1996, **45**, 17–20.
40 S. W. J. Lamberts, A.-J. van der Lely, W. W. de Herder and L. J. Hofland, *N. Engl. J. Med.*, 1996, **334**, 246–254.
41 M. Maeder and P. King, *ReactLab*, Jplus Consulting Pty Ltd: East Fremantle, WA. Australia, 2009.
42 R. A. Binstead, A. D. Zuberbuhler and B. Jung, *SPECFIT32, 3.0.34; Spectrum*, Software Associates, Marlborough, MA, USA, 2005.
43 M. A. Gonzálvez, A. Gallen, M. Ferrer and M. Martínez, *Inorg. Chem.*, 2020, **59**, 1582–1587.